Neuropsychopharmacology (2011) 36, 2498–2512

www.neuropsychopharmacology.org

Acute Nicotine-Induced Tachyphylaxis Is Differentially Manifest in the Limbic System

Yantao Zuo[1,4], Hanbing Lu[1], D Bruce Vaupel[1], Yi Zhang[2], Svetlana I Chefer[1], William R Rea[1], Anna V Moore[3], Yihong Yang[1] and Elliot A Stein[1]

[1]Neuroimaging Research Branch, National Institute on Drug Abuse, Intramural Research Program, Baltimore, MD, USA; [2]National Institute on Mental Health, Bethesda, MD, USA; [3]Molecular Imaging Laboratory, Department of Radiology, MGH/MIT/HMS Athinoula A Martinos Center for Biomedical Imaging, Massachusetts General Hospital, Charlestown, MA, USA

Rapid tolerance develops to many of nicotine's behavioral and autonomic effects. A better understanding of the spatiotemporal patterns in neuronal activity as a consequence of acute nicotine tolerance (tachyphylaxis) may help explain its commonly found inverted 'U'-shaped biphasic dose–effect relationship on various behaviors. To this end, we employed high-resolution functional magnetic resonance imaging and relative cerebral blood volume (rCBV) as a marker of neuronal activity, to characterize the regional development of acute tolerance as a function of nicotine dose in naïve, anesthetized rats. A single intravenous nicotine injection at 0.1 and 0.3, but not 0.03 mg/kg, significantly increased neuronal activity in many neocortical areas. In contrast, dose-dependent increases in rCBV were most pronounced in limbic regions, such that responses seen at 0.1 mg/kg nicotine in accumbens, hippocampus, amygdala, and several other limbic areas were not seen following 0.3 mg/kg nicotine. Finally, whereas profound tolerance was observed in many cortical regions after the second of two paired nicotine injections at either 0.1 or 0.3 mg/kg, subcortical limbic structures showed only a weak trend for tolerance. Lack of rCBV changes in animals receiving nicotine methiodide, a quaternary nicotine analog that does not cross the blood–brain barrier, supports a direct neuronal effect of nicotine rather than an action on the vasculature. These data provide pharmacodynamic insight into the regional heterogeneity of nicotine tachyphylaxis development, which may be relevant to behavioral and neurobiological mechanisms associated with repeated tobacco consumption.
Neuropsychopharmacology (2011) **36,** 2498–2512; doi:10.1038/npp.2011.139; published online 27 July 2011

Keywords: phMRI; nicotine; tolerance; relative cerebral blood volume

INTRODUCTION

Nicotine is the primary chemical constituent in tobacco responsible for its addictive properties. Both acute (tachyphylaxis) and chronic tolerance to nicotine are implicated in mechanisms of tobacco dependence (Perkins *et al*, 1993, 2002; Pomerleau *et al*, 1993). To the extent that dysfunctional nicotinic cholinergic transmission is involved in various neuropsychiatric diseases (Dani and Bertrand, 2007; Newhouse *et al*, 1997; Perry *et al*, 2000), understanding the neurobiological mechanisms underlying tolerance to nicotinic acetylcholine receptor (nAChR) activation seems essential for the development of therapeutic strategies to treat these pathological conditions (eg, Maelicke and Albuquerque, 1996), the central sites of which are still poorly understood.

Nicotinic ligand-gated ion channels in mammalian brain are pentameric structures consisting of diverse subunits, $\alpha2$–$\alpha6$ and $\beta2$–$\beta4$ for $\alpha\beta$ heteromeric types and $\alpha7$ for homomers. The assembled subunit stoichiometry dictates varied receptor functional properties such as ion permeability, receptor–ligand binding affinity, desensitization, and upregulation. At a systems level, the differential expressions of nAChR subtypes on diverse neuronal populations and locations are hypothesized to contribute to their regional- and circuit-specific roles in modulating synaptic transmission (Albuquerque *et al*, 2009; Dani and Bertrand, 2007). As nicotine has a distinct binding affinity for specific receptor subtypes, each of which is also characterized by its own desensitization rate, nAChRs are sensitive to varied nicotine concentrations over finite intervals, which likely contribute to its dose-dependent effects on motivated behaviors (eg, Corrigall and Coen, 1989; Le Foll and Goldberg, 2005; Le Foll *et al*, 2007) and cognition (Levin *et al*, 1998, 2006; Levin and Chen, 2004). Furthermore, nicotine dose is known to affect desensitization rates of nAChRs (Dani *et al*, 2000; Ochoa *et al*, 1989,

Correspondence: Dr EA Stein, National Institute on Drug Abuse Intramural Research Program (NIDA IRP), Neuroimaging Research Branch, 251 Bayview Boulevard, Suite 200, Room 7A711A, Baltimore, MD 21224, USA, Tel: +1 443 740 2650, Fax: +1 443 740 2734, E-mail: estein@mail.nih.gov
[4]Current address: Department of Psychiatry and Behavioral Sciences, Center for Nicotine and Smoking Cessation Research, Duke University Medical Center, Durham, NC, USA
Received 24 March 2011; revised 16 June 2011; accepted 18 June 2011

1990). Critically, for this study, not only are nicotine's behavioral and cognitive effects dose-dependent, but tolerance is also differentially expressed across these measures. For example, robust acute tolerance develops to many aversive drug effects (eg, head rush and jitteriness), whereas little or weak tolerance is seen to stimulating (eg, vigor and arousal), attention-enhancing, and pleasant behavioral properties (eg, calmness and happiness) of nicotine in human smokers (Perkins *et al*, 1994; Warburton and Mancuso, 1998). Understanding nicotine-induced regional and circuit-specific tolerance properties could provide mechanistic explanations for the differential development of tolerance across behavioral domains.

The application of functional magnetic resonance imaging (fMRI) techniques to neuropharmacology, termed pharmacological MRI (phMRI), has been used to image dynamic drug-induced changes throughout the brain. phMRI typically employs the traditional BOLD (blood oxygen level-dependent) signal or, more recently, cerebral blood volume (CBV) or cerebral blood flow (CBF) signals, all of which reflect neuronal activity (Logothetis *et al*, 2001; Sheth *et al*, 2003; Smith *et al*, 2002). With these hemodynamic methods, it is possible to visualize or 'map' temporal and spatial changes elicited by nicotine simultaneously in multiple brain regions within a single study or longitudinally with different experimental designs (Leslie and James, 2000; Martin and Sibson, 2008; Stein *et al*, 1998).

In this study, we employed CBV-weighted phMRI to identify those regions and neuronal systems that exhibit acute tolerance to repeated nicotine administration. CBV phMRI was selected because its sensitivity is superior to that of the BOLD technique (Lu *et al*, 2004; Sheth *et al*, 2003). We employed paired nicotine injections at various doses to characterize the spatiotemporal profiles of rapid tolerance development in drug-naïve, anesthetized rodents. Our data demonstrate that nicotine tachyphylaxis develops differentially and dose-dependently in cortical *vs* subcortical limbic regions.

MATERIALS AND METHODS

Animal Preparation and Physiological Measurements

A total of 30 male Sprague–Dawley rats (Charles River, Wilmington, MA) weighing 300–380 g were surgically prepared and imaged using procedures approved by the Animal Care and Use Committee of the National Institute on Drug Abuse Intramural Research Program. Animals were pair-housed under a 12-h light/dark cycle (0600 hours lights on) with *ad libitum* access to food and water.

On test days, rats were anesthetized with 2% isoflurane in a 1 : 1 mixture of O_2 : air and glycopyrrolate (0.5 mg/kg, subcutaneously); a peripherally acting quaternary muscarinic antagonist was administered to prevent airway blockade by minimizing secretory activity. Both femoral veins and one femoral artery were catheterized with PE-50 tubing for drug delivery and monitoring arterial blood gases and blood pressure, respectively. The wound area and incision were infiltrated with the long-lasting local anesthetic Marcaine and closed.

Animals were intubated and transferred to a customized animal holder with their heads secured with a mouth clamp and ear bars, placed on artificial ventilation, and positioned within the center of the magnet for imaging. The peripherally acting quaternary neuromuscular blocker pancuronium bromide was administered (loading dose, 2.0 mg/kg followed by continuous intravenous infusion at 2.0 mg/kg/h) to minimize motion artifacts. Core body temperature was maintained at 37 °C with a circulating water heating pad throughout all procedures. End tidal CO_2 and O_2, heart rate, blood pressure, and temperature were monitored continuously. Arterial blood gases were assessed intermittently and maintained within normal physiological limits (pCO_2, 35–45 (mean 39.5) mm Hg; pO_2, >110 mm Hg). Throughout fMRI data acquisition, a stable anesthetic level was maintained with 1.7–1.8% isoflurane mixed with air containing 30% oxygen.

phMRI Paradigm

Animals were assigned to one of five groups ($n = 6$ per group). Group 1 (Sal) received two saline injections. Groups 2–4 received, respectively, two consecutive injections of 0.03, 0.10, or 0.30 mg/kg intravenous nicotine hydrogen tartrate (Sigma-Aldrich, St Louis, MO; pH titrated to 7.4 with NaOH, doses expressed as free base). Doses were selected from literature values reflecting a low and effective self-administered dose (0.03 mg/kg; eg, Corrigall and Coen, 1991) to moderate and higher doses associated with various dose-dependent behavioral effects (Matta *et al*, 2007). A fifth group was injected twice with a dose of the quaternary nicotine analog nicotine pyrrolidine methiodide (hereafter referred to as nicotine methiodide) equal to 0.30 mg/kg nicotine free base in molar concentration (1.85 mM). As nicotine methiodide possesses the pharmacological properties of nicotine, but does not pass the blood–brain barrier (Aceto *et al*, 1983), it allowed us to disambiguate true CNS relative CBV (rCBV) responses from those that might result from activation of peripheral nAChRs that alter autonomic responses (eg, increases in heart rate, blood pressure, respiration), which could independently and nonspecifically alter rCBV. Nicotine methiodide was synthesized in our lab (see Supplementary Materials). Experiments adhered to a 1-h timeline in which a 10-min baseline preceded the first injection, and a second, identical injection was administered 25 min later, followed by a final 25 min observation period. Drug or saline challenges were injected using an infusion pump in an identical manner: 1.0 ml/kg over 30 s.

fMRI Scanning Procedures

MRI data were acquired using a Bruker Biospin 9.4T scanner (Bruker Medizintechnik, Karlsruhe, Germany). A birdcage coil was used for RF excitation and a surface coil for signal reception. The anterior commissure (−0.36 mm from bregma, coronal view) was used as the landmark for slice localization. Following animal preparation (45 min), high-resolution T_2-weighted structural images were obtained over 4 min using a rapid acquisition with relaxation enhancement (RARE) sequence (echo time (TE) 12.5 ms, repetition time (TR) 2520 ms, RARE factor 8, field of view (FOV) = $3.5 \times 3.5\,cm^2$, 23 slices of 1.0 mm thickness) and were subsequently used for functional image registration. This procedure was followed by a 5-min MRI

scan (Lu *et al*, 2008) during which MION (Ferumoxtran-10, 20 mg/kg intravenous injection time −1 min) was given after a 2-min baseline period. For this scan, a conventional gradient echo (GE) sequence was used with the following parameters: FOV = $3.5 \times 3.5\,cm^2$, matrix size 96×96, 13 slices of 1.0 mm thickness, TR/TE = 313/5.4 ms. After 10 min, a second 5-min MION (5 mg/kg intravenous) scan/administration was acquired to optimize the rCBV-weighted signal (Lu *et al*, 2007). The next scan consisted of the phMRI component. To achieve whole brain spatial coverage with minimal geometric distortions and signal drop out, we employed a GE sequence to collect 120 volumes of imaging data with parameters identical to those used in the MION injection scan. This sequence facilitated group level data analysis, but at the cost of relatively low temporal resolution (30 s per volume). However, even with this limited temporal resolution, we were able to analyze kinetic parameters of drug activation responses, as their time courses were sufficiently long (approximately 5 min). Blood gas samples were acquired before and after the scan sequence.

MRI Data Analysis

MRI data processing and analyses were performed using AFNI (Cox, 1996) supplemented by MATLAB (MathWorks, Natick, MA). Structural images from a randomly chosen animal served as a template, and images from all other rats were co-registered to this common space using a method developed by Lu *et al* (2010). Briefly, fiducial tags were placed on 10 distinct anatomical landmarks in high-resolution structural images and an alignment routine in AFNI was executed to co-register all structural images. A transformation matrix generated for the co-registration of structural brain images from an individual animal was also applied to align functional images from the same animal. Fine adjustments were made manually as necessary.

Relative CBV changes in each voxel during the 1-h phMRI experiments were calculated based on pre- and post-MION baseline signal intensities (Mandeville *et al*, 1998),

$$rCBV(t) = \log(S_{raw(t)}/S_{post})/\log(S_{post}/S_{pre}) \quad (1)$$

where S_{pre} and S_{post} are pre-MION and post-MION baseline signal intensity, and S_{raw} is raw signal at time t of the 1-h scan.

The rCBV images were then smoothed using a three-dimensional Gaussian kernel with full-width half-maximum of 0.4 mm. Because each of the two rCBV time-course responses produced by the paired drug or saline challenges returned to baseline within 15 min, the original 1-h time course was divided into two segments, each corresponding to one injection. This division improved the removal of linear and quadratic trend noise during nonlinear fitting of the rCBV time courses compared with fitting the two drug-induced responses simultaneously. The rCBV time courses in individual voxels were fitted with a difference of two exponential function curves to represent the following pharmacokinetic profile of drug action:

$$y(t) = k(e^{-\alpha_1(t-t_0)} - e^{-\alpha_2(t-t_0)})\ t \geq t_0 \quad (2)$$

where t_0 is the response starting point, k is the multiplicative coefficient, α_1 is the elimination rate, and α_2 is the absorption rate. The initial values used to fit parameters t_0, k, α_1, and α_2 were: 0–1 min after drug/saline administration, −40 to 40, 0–0.5, and 0.51–10.0, respectively, and were estimated after visual inspection of voxel time courses across all animals. The optimum solution was found using the program DiffExp in AFNI (Cox, 1996). This program started with a random search of 100 parameter vectors followed by nonlinear optimizations using the simplex algorithm so that the final solution of Equation (2) was a least-square estimation of the original time course. Half-times for the ascending and descending components of the rCBV time course were calculated by identifying the maximum response values, followed by numerical calculation of the times to reach half-maximum of the rising and trailing phases, respectively.

Statistical Analysis

Peak amplitude of the rCBV response was the primary index of drug-induced brain activation. A 4 (DOSE) × 2 (INJECTION) ANOVA tested for dose- and injection-dependent effects of nicotine. A similar voxel-based 2 (DOSE) × 2 (INJECTION) ANOVA was used to examine differences between the nicotine methiodide and saline groups. *Post hoc* analyses were conducted to identify significant differences among groups and/or consecutive injections as indicated by ANOVA. Significance threshold for all analyses was set at $p_{corrected} < 0.005$, with a minimum cluster size of 14 voxels as determined using Monte Carlo simulation calculated with the AlphaSim module of AFNI.

In all, 24 atlas-defined anatomical ROIs (Paxinos and Watson, 2005) were co-registered to high-resolution anatomical MR images (Lu *et al*, 2010) to cover most major cortical and subcortical regions (Figure 1), and used as masks to extract regional activation. For each subject, a single rCBV peak amplitude was calculated within each ROI by averaging the signals from voxels comprising the overlapped anatomical and functional ROIs and subjected to ANOVA. For subsequent group comparisons, significance level was set at $p < 0.05$ after Bonferroni correction. To further characterize temporal patterns of brain activation, voxel-wise 4 (DOSE) × 2 (INJECTION) ANOVAs and *post hoc* analyses were conducted for latency to peak effect and half-time for the ascending and descending phases of the rCBV time courses.

Mean arterial blood pressure (MAP) recorded during the 1-h phMRI experiment was normalized to the average of the 10-min baseline period for each experiment. MAP peak responses for treatment groups were subjected to a 5 (GROUP; now including nicotine methiodide) × 2 (INJECTION) ANOVA with follow-up group comparisons similar to the rCBV data.

RESULTS

There were significant main effects of DOSE and INJECTION and a DOSE × INJECTION interaction on rCBV peak amplitude (Figures 2a–c). Subsequent *post hoc* *t*-tests revealed a mostly inverted U-shaped dose–response effect (Figures 3a–c and 4). Notably, while there was no difference between the saline and the low-dose 0.03 mg/kg nicotine groups (Figure 3a), maximal neuronal effects were seen

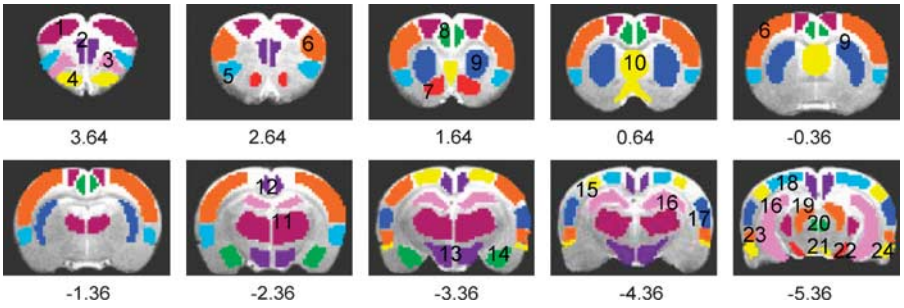

Figure 1 Definition of anatomical region of interest (ROI) placements, superimposed on coronal slices through the rat neuraxis (Paxinos and Watson, 2005). A digital rat brain atlas superimposed onto corresponding structural images guided ROI drawing. (1) Motor cortex; (2) medial prefrontal cortex (mPFC); (3) orbital cortex; (4) olfactory bulb (including olfactory tubercle and piriform cortex); (5) insula; (6) somatosensory cortex; (7) nucleus accumbens; (8) cingulate cortex; (9) caudate and putamen; (10) septum; (11) thalamus; (12) retrosplenial dysgranular and granular cortices (RSDG); (13) hypothalamus; (14) amygdala; (15) parietal cortex; (16) hippocampus; (17) auditory cortex; (18) visual cortex; (19) brain stem; (20) periaqueductal gray; (21) ventral tegmental area (VTA); (22) substantia nigra; (23) perirhinal cortex; and (24) entorhinal cortex. Numbers below images indicate slice locations (mm) relative to bregma. Functionally activated ROIs within these anatomically defined ROIs were based on whole brain, voxel-based analyses.

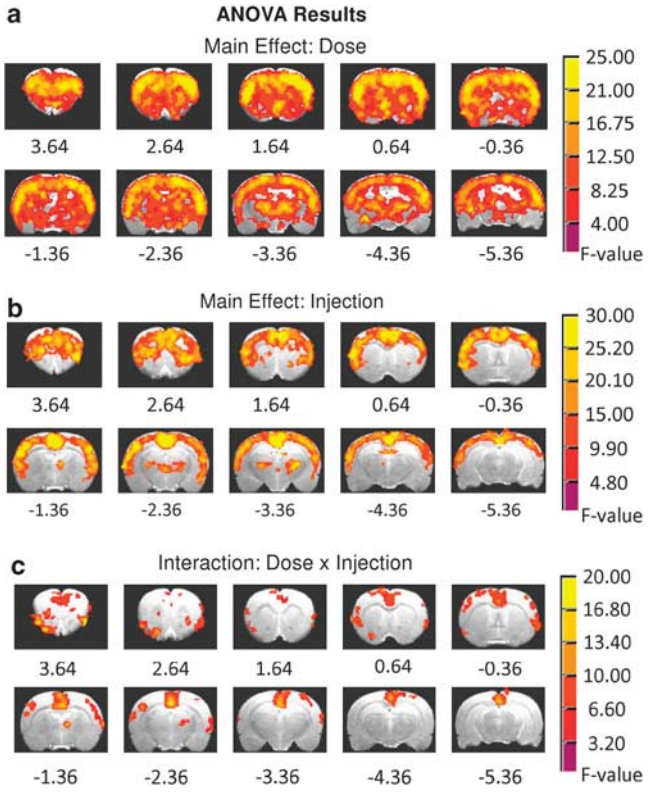

Figure 2 Summary of voxel-based analysis of variance (ANOVA) results. Peak relative cerebral blood volume (rCBV) responses to the nicotine and saline injections in each voxel were evaluated with 4 (DOSE) × 2 (INJECTION) factor ANOVAs. Activated voxels were thresholded for each factor and the interaction effect at $p_{corrected} < 0.005$. (a) The DOSE main effect of nicotine (0 (saline), 0.03, 0.10, and 0.30 mg/kg) demonstrated widespread brain activation. (b) The INJECTION main effect, which indicates the development of tolerance, is illustrated for the two consecutive injections spaced 25 min apart for either saline or the three doses of nicotine. (c) Significant DOSE × INJECTION interactions were regionally restricted.

following the middle 0.1 mg/kg nicotine (Figure 3b). The biphasic pattern is most apparent from the statistical difference map between the high, 0.3, and middle, 0.1 mg/kg doses (Figure 3c). Unique characteristics of the dynamic nature of the DOSE × INJECTION interaction become apparent when examining the effects of each injection separately as discussed below.

Dose-Dependent and Region-Specific Effects of the First Nicotine Injection

Significant dose-dependent activation was seen in 20 of the 24 *a priori* anatomical ROIs. The four remaining unaffected ROIs, entorhinal cortex, periaqueductal gray, substantia nigra, and VTA, were excluded from further analysis. The 0.03 mg/kg nicotine dose, like saline, produced negligible changes in rCBV. However, at 0.1 and 0.3 mg/kg, nicotine significantly increased rCBV in primary sensory and motor cortices and limbic cortical areas such as mPFC, orbital, cingulate, and retrosplenial dysgranular and granular cortices (RSDG) (Table 1 and Figures 4a and c), with the greatest activation magnitude in these regions most often seen after the middle dose. Subcortical areas (Table 1) including caudate–putamen, thalamus (Figures 4a and c), and brain stem structures showed a pattern similar to cortical regions, although the highest dose of nicotine elicited smaller response increases.

In contrast to the above spatiotemporal pattern, rCBV responses in subcortical limbic areas, including the septum, hippocampus, amygdala, nucleus accumbens (NAc), olfactory bulb, and hypothalamus, revealed profound dose-dependent and region-specific responses to nicotine (Table 1). In these subcortical areas, 0.1 mg/kg nicotine tended to induce smaller rCBV increases than in the majority of activated cortical regions. More strikingly, and in contrast to the rCBV increases produced by 0.1 mg/kg nicotine in limbic regions, 0.3 mg/kg nicotine induced little change in such limbic regions as NAc, hippocampus (Figure 4a), and amygdala (Table 1 and Figures 4a and c). Therefore, nicotine induced a robust inverted U-shaped dose-dependent activation effect within most subcortical limbic, but not cortical, regions.

Pharmacokinetic Parameters

There was a significant main effect of DOSE for both latency to peak effect and time to half-maximum of the ascending

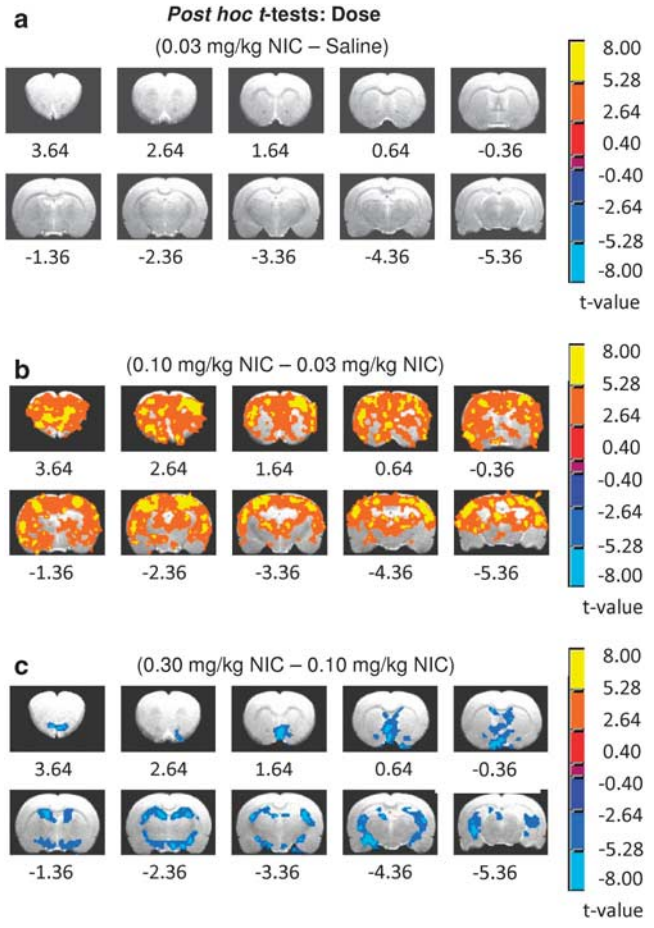

Figure 3 Difference maps for the *post hoc t*-tests for the DOSE main effect showing the dose-dependent effects of nicotine (NIC) on relative cerebral blood volume (rCBV) peak amplitude. Voxels in each of these *t*-maps were thresholded for group comparisons at $p_{corrected} < 0.005$. (a) The lowest dose of nicotine tested was without effect and thus was functionally equivalent to saline. (b) Effects of 0.10 mg/kg NIC compared with 0.03 mg/kg NIC were widespread and represent the apogee of the inverted U-shaped dose–effect curve. (c) The blue colors in this contrast map indicate decreases in activation between the high and middle NIC doses, suggesting a less efficacious action as dose increased, comprising the right (falling) side of an inverted U-shaped dose–response relationship.

rCBV response, but no INJECTION or DOSE × INJECTION interaction. In contrast, there were no significant differences when considering half-time of the descending phase of the rCBV time courses. Further, *post hoc* analyses of the peak latency and ascending half-times revealed fairly homogeneous spatial results (Supplementary Tables S1 and S2), with the latency to peak effect consistently, although not universally, longest for 0.1 mg/kg nicotine in all ROIs showing a nicotine DOSE effect (Supplementary Table S1). This pattern was most pronounced in subcortical limbic areas, including septum, hippocampus, and hypothalamus (Supplementary Table S1). Similarly, ascending half-times were consistently greater for the 0.1 mg/kg dose in contrast to those for the other DOSE groups (Supplementary Table S2). Taken together, these data suggest that the intermediate, 0.10 mg/kg dose was associated with the longest response time to reach peak efficacy.

Acute Tolerance to Nicotine is Dose-Dependent and Region-Specific

Repeated nicotine administration induced profound tachyphylaxis development. Figures 4b and c and Table 2 depict the time courses and biphasic nature of the peak effects as well as the tolerance profiles associated with the repeated nicotine injections. Significant main effects of INJECTION (ie, tolerance) were seen in primary sensory/motor cortices, limbic-related cortical areas, and subcortical regions such as caudate–putamen and thalamus. Among subcortical limbic structures for which we observed dose-dependent nicotine effects (Table 1), only the hippocampus exhibited modest tolerance (Table 2). *Post hoc* analysis revealed that tachyphylaxis was most pronounced following the second 0.30 mg/kg dose (ie, 14/14 regions showed significant differences at 0.30 mg/kg and 7/14 regions in the 0.10 mg/kg group; Table 2). Indeed, tachyphylaxis seen at the high nicotine dose was so profound that the rCBV response after the second injection approached the nominal changes observed with saline and 0.03 mg/kg nicotine. In contrast, attenuated responses to the second 0.10 mg/kg nicotine injection relative to the first were seen in motor and parietal cortices and several limbic-related cortical areas, whereas nonsignificant trends were seen in the sensory cortices, perirhinal cortex, caudate–putamen, and thalamus (Table 2 and Figure 4).

Table 3 and Figure 2c summarize the significant DOSE × INJECTION interactions. *Post hoc* analyses demonstrated marked rCBV reductions between the first and second nicotine injections at the 0.1 and 0.3 mg/kg doses within somatosensory, insula and motor cortices, and limbic cortices, including orbital, cingulate, RSDG, olfactory areas, and the thalamus. In contrast, data presented in Table 2 and Figure 4 suggest little or no tolerance development in the high-dose nicotine group within the septum, amygdala, NAc, and hypothalamus, and smaller, although still significant tolerance in the hippocampus (Table 2). There were few signs of tolerance development associated with the middle nicotine dose in these subcortical limbic regions (Tables 1 and 2), nor was tolerance seen in the brain stem (Table 2). Thus, both the main effects of INJECTION and the DOSE × INJECTION interactions for peak rCBV amplitudes revealed rapid, acute tolerance development for both 0.10 and 0.30 mg/kg doses in many cortical regions, with weaker effects seen in subcortical limbic structures.

Differentiating the Peripheral and Central Effects of Nicotine Using Nicotine Methiodide

As the characteristic vasopressor response of nicotine may potentially contribute to and confound the CBV measurements, we administered a unique quaternary nicotine analog in a separate group of animals. ANOVA of the peak MAP increases expressed as a percentage of baseline demonstrated a significant GROUP effect ($p < 0.001$), but no INJECTION or GROUP × INJECTION interaction. Owing to the lack of tolerance on MAP (ie, a nonsignificant INJECTION factor), *post hoc* group comparisons were performed on the average peak MAP change for each pair of injections. Critically, there was no difference in peak MAP response for equimolar concentrations of nicotine

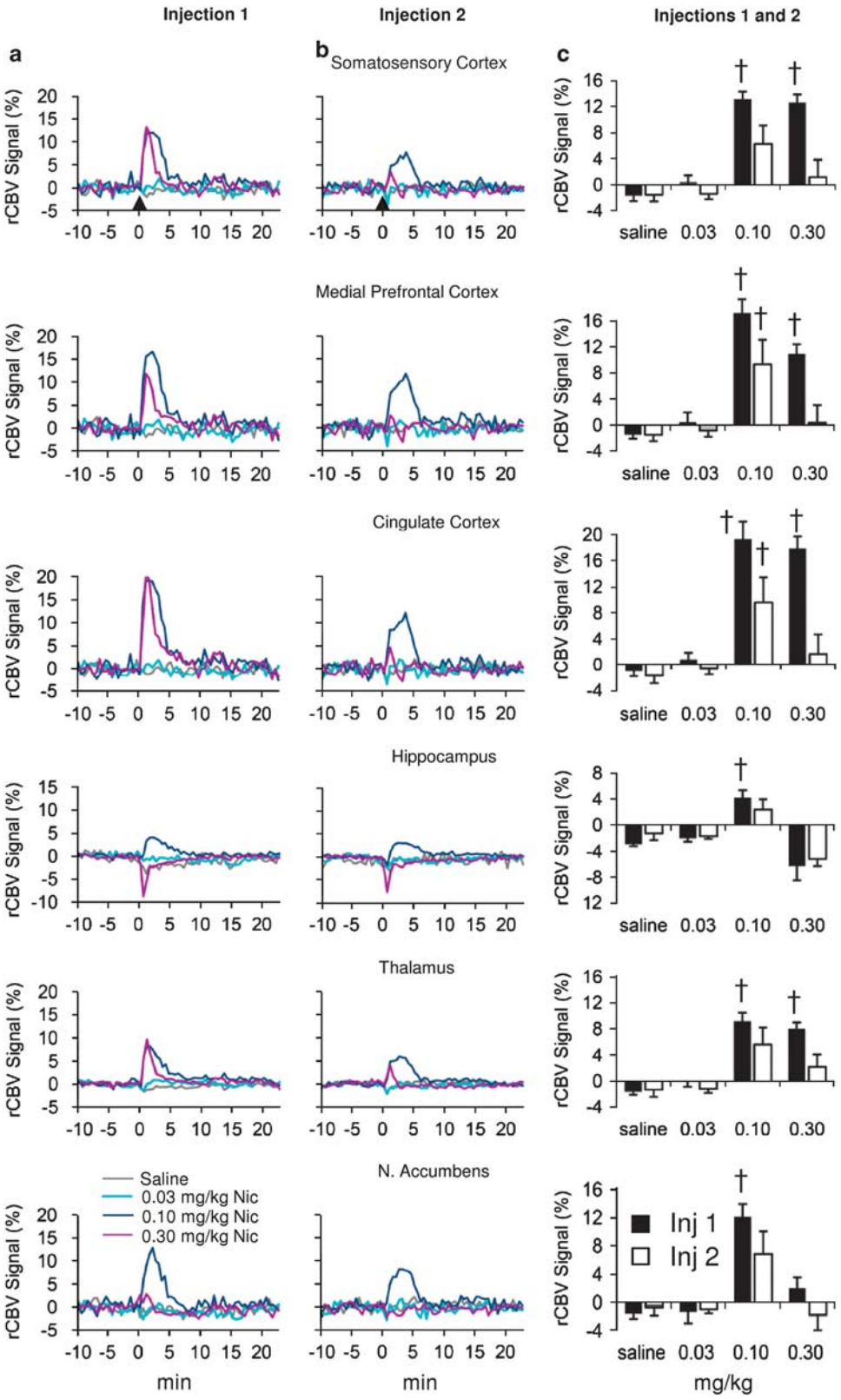

Figure 4 Relative cerebral blood volume (rCBV) time courses and peak responses in selected brain regions demonstrating acute nicotine tolerance development as a function of DOSE and INJECTION. Injections were spaced 25 min apart. Signal intensity values, expressed as a percent change of the preinjection baseline for each group, were averaged across activated voxels in each region of interest (ROI) as identified by analysis of variance (ANOVA). Columns (a) and (b) show the time courses for the first and second injections, respectively. Column (c) bar graphs present the mean peak amplitudes ± SEM of the respective fitted time courses for injections shown in columns (a) and (b). (†) Signifies a difference from the saline condition ($p < 0.05$ after Bonferroni correction). All injections occurred at time 0, shown by black arrow in columns (a) and (b).

Table 1 Dose–Response Effects of Nicotine on rCBV

Area (number of voxels)	Group				Group differences
	1	2	3	4	
	Saline	0.03 mg/kg	0.10 mg/kg	0.30 mg/kg	
Primary cortex					
Auditory	−1.73 ± 1.08[a]	−0.01 ± 1.26	14.68 ± 1.41	13.03 ± 1.90	3>1, 2; 4>1, 2
(204)	−2.17 ± 1.01[b]	−1.90 ± 1.33	7.26 ± 3.44	1.40 ± 3.07	
Visual	−1.60 ± 1.00	−0.25 ± 1.09	14.48 ± 1.53	12.03 ± 1.79	3>1, 2; 4>1, 2
(135)	−1.57 ± 1.21	−1.77 ± 1.00	7.30 ± 3.22	2.15 ± 3.12	
Somatosensory	−1.67 ± 0.86	0.42 ± 1.04	13.14 ± 1.16	12.63 ± 1.24	3>1, 2; 4>1, 2
(1379)	−1.56 ± 1.03	−1.39 ± 0.87	6.30 ± 2.78	1.16 ± 2.68	
Insula	−1.81 ± 0.93	0.49 ± 1.24	16.85 ± 1.71	14.44 ± 1.34	3>1, 2; 4>1, 2
(350)	−1.47 ± 0.97	−1.38 ± 0.93	8.14 ± 3.87	0.77 ± 3.06	
Motor	−1.45 ± 1.01	0.53 ± 0.98	15.06 ± 1.79	10.73 ± 1.09	3>1, 2; 4>1, 2
(560)	−0.21 ± 0.99	−0.89 ± 0.65	7.21 ± 2.99	0.11 ± 2.71	
Parietal	−1.55 ± 1.05	−0.24 ± 1.02	14.13 ± 1.48	11.60 ± 1.61	3>1, 2; 4>1, 2
(151)	−1.55 ± 1.09	−1.69 ± 0.90	6.94 ± 2.99	1.72 ± 2.96	
Limbic cortex					
mPFC	−1.52 ± 0.60	0.44 ± 1.51	17.20 ± 2.15	10.91 ± 1.48	3>1, 2; 4>1, 2
(104)	−1.52 ± 0.98	−0.85 ± 0.97	9.30 ± 3.81	0.36 ± 2.69	3>1, 2
Orbital	−2.04 ± 0.65	−0.42 ± 1.16	13.11 ± 1.06	7.32 ± 1.65	3>1, 2, 4; 4>1, 2
(178)	−0.05 ± 0.92	−1.23 ± 0.63	5.77 ± 2.46	−1.07 ± 2.81	
Cingulate	−1.07 ± 0.76	0.82 ± 1.06	19.31 ± 2.71	17.85 ± 1.88	3>1, 2; 4>1, 2
(125)	−1.75 ± 1.17	−0.67 ± 0.87	9.60 ± 3.86	1.68 ± 3.03	3>1
RSDG	−1.80 ± 0.62	0.25 ± 0.67	14.54 ± 2.28	14.75 ± 2.00	3>1, 2; 4>1, 2
(135)	−1.36 ± 1.04	−1.37 ± 0.51	7.57 ± 3.30	1.54 ± 2.88	
Perirhinal	−3.24 ± 1.31	−1.25 ± 1.22	14.14 ± 2.63	11.03 ± 1.46	3>1, 2; 4>1, 2
(59)	−2.46 ± 0.92	−1.64 ± 1.54	7.55 ± 4.24	0.91 ± 3.00	
Olfactory bulb	−2.24 ± 0.89	−3.64 ± 1.23	9.85 ± 1.13	−0.44 ± 0.96	3>1, 2, 4
(157)	−0.04 ± 0.74	−1.79 ± 0.30	4.51 ± 1.89	−3.15 ± 1.40	3>2, 4
Subcortical limbic system					
Septum	−2.10 ± 0.43	−1.90 ± 1.04	8.25 ± 1.48	−2.61 ± 1.75	3>1, 2, 4
(222)	−0.08 ± 0.96	−2.02 ± 0.39	5.12 ± 2.28	−3.05 ± 1.44	3>2, 4
Hippocampus	−2.92 ± 0.30	−1.97 ± 0.56	4.23 ± 1.13	−6.31 ± 2.17	3>1, 2, 4
(356)	−1.26 ± 1.03	−1.69 ± 0.40	2.38 ± 1.58	−5.16 ± 1.13	
Amygdala	−3.70 ± 0.97	−0.56 ± 1.39	12.67 ± 2.54	−0.57 ± 1.64	3>1, 2, 4
(32)	−0.79 ± 1.39	−2.29 ± 0.83	8.76 ± 3.90	−4.64 ± 1.99	3>2, 4
Accumbens	−1.62 ± 0.77	−1.32 ± 1.65	12.23 ± 1.80	2.06 ± 1.47	3>1, 2, 4
(105)	−0.67 ± 1.18	−0.97 ± 0.58	6.87 ± 3.20	−1.78 ± 2.20	3>4
Hypothalamus	−2.80 ± 0.47	−1.72 ± 1.02	3.78 ± 1.22	−1.09 ± 1.10	3>1, 2, 4
(134)	−1.24 ± 1.25	−1.86 ± 0.59	4.36 ± 2.03	−3.02 ± 0.89	3>1, 2, 4
Caudate–putamen	−1.29 ± 0.66	0.01 ± 1.36	10.56 ± 1.12	4.92 ± 0.93	3>1, 2, 4; 4>1, 2
(638)	−2.05 ± 1.22	−1.61 ± 1.07	5.31 ± 3.53	−0.74 ± 1.76	
Thalamus	−1.65 ± 0.45	−0.15 ± 0.73	9.17 ± 1.31	8.03 ± 0.95	3>1, 2; 4>1, 2
(722)	−1.34 ± 1.11	−1.21 ± 0.61	5.63 ± 2.55	2.19 ± 1.90	
Brain stem	−0.88 ± 1.04	−1.00 ± 0.68	6.16 ± 1.12	3.64 ± 0.86	3>1, 2; 4>1, 2
(71)	−0.93 ± 1.06	−1.74 ± 0.39	5.51 ± 2.26	1.20 ± 1.48	3>1, 2

Abbreviations: mPFC, medial prefrontal cortex; RSDG, retrosplenial dysgranular and granular cortices.
Values represent percent rCBV changes relative to the baseline for each of the two injections. The upper and lower values represent the 1st and 2nd injections as shown by the exemplary superscripts a and b, respectively. Significant group differences were thresholded at $p < 0.05$ after Bonferroni correction. Values represent the mean ± SEM for each treatment group ($n = 6$ per group).

Table 2 Regions Developing Nicotine Tachyphylaxis

Area (number of voxels)	Group				Group differences
	1	2	3	4	
	Saline	0.03 mg/kg	0.10 mg/kg	0.30 mg/kg	
Primary cortex					
Auditory	−1.55 ± 1.20[a]	0.30 ± 1.23	14.90 ± 1.39	13.40 ± 1.96	4a > 4b
(158)	−2.44 ± 1.10[b]	−1.97 ± 1.30	7.37 ± 3.44	1.45 ± 3.10	
Visual	−1.58 ± 1.01	−0.25 ± 1.11	14.71 ± 1.55	12.32 ± 1.80	4a > 4b
(125)	−1.56 ± 1.18	−1.74 ± 1.00	7.39 ± 3.26	2.22 ± 3.16	
Somatosensory	−1.61 ± 0.85	0.48 ± 1.06	13.20 ± 1.15	12.81 ± 1.25	3a > 3b; 4a > 4b
(1281)	−1.60 ± 1.01	−1.41 ± 0.89	6.30 ± 2.78	1.17 ± 2.69	
Insula	−1.63 ± 0.96	0.72 ± 1.21	16.85 ± 1.69	14.65 ± 1.34	4a > 4b
(306)	−1.40 ± 0.97	−1.50 ± 0.97	7.91 ± 3.81	0.72 ± 3.03	
Motor	−1.23 ± 0.90	0.73 ± 1.07	15.35 ± 1.94	11.26 ± 1.12	3a > 3b; 4a > 4b
(431)	−0.66 ± 1.00	−1.01 ± 0.71	7.26 ± 3.12	0.35 ± 2.72	
Parietal	−1.49 ± 1.03	−0.18 ± 1.01	14.23 ± 1.49	11.59 ± 1.58	3a > 3b; 4a > 4b
(143)	−1.49 ± 1.05	−1.66 ± 0.87	6.96 ± 2.98	1.71 ± 2.95	
Limbic cortex					
mPFC	−1.23 ± 0.90	0.73 ± 1.07	15.35 ± 1.94	11.26 ± 1.12	3a > 3b; 4a > 4b
(80)	−0.66 ± 1.00	−1.00 ± 0.71	7.26 ± 3.12	0.35 ± ± 2.72	
Orbital	−1.88 ± 0.67	−0.27 ± 1.24	13.70 ± 1.15	8.62 ± 1.55	3a > 3b; 4a > 4b
(124)	−0.03 ± 0.91	−1.45 ± 0.75	6.00 ± 2.54	−0.94 ± 2.89	
Cingulate	−1.07 ± 0.76	0.82 ± 1.06	19.31 ± 2.71	17.85 ± 1.88	3a > 3b; 4a > 4b
(125)	−1.75 ± 1.17	−0.67 ± 0.87	9.60 ± 3.86	1.68 ± 3.03	
RSDG	−1.82 ± 0.62	0.23 ± 0.66	14.37 ± 2.29	14.58 ± 2.01	3a > 3b; 4a > 4b
(138)	−1.39 ± 1.04	−1.37 ± 0.50	7.50 ± 3.28	1.50 ± 2.86	
Perirhinal	−1.98 ± 1.46	−0.02 ± 1.55	15.12 ± 2.40	12.19 ± 1.09	4a > 4b
(22)	−2.68 ± 0.85	−2.14 ± 1.95	7.15 ± 4.22	0.88 ± 3.08	
Subcortical limbic system					
Hippocampus	−3.33 ± 0.36	−2.25 ± 0.50	1.94 ± 0.79	−6.60 ± 1.18	1b > 1a; 4b > 4a
(18)	−0.94 ± 0.85	−2.22 ± 0.53	−0.18 ± 0.59	−3.63 ± 0.49	
Caudate–putamen	−0.91 ± 0.70	0.45 ± 1.51	11.62 ± 1.35	5.85 ± 0.69	4a > 4b
(68)	−2.47 ± 1.06	−1.94 ± 1.09	5.71 ± 3.59	−1.05 ± 1.90	
Thalamus	−1.72 ± 0.46	0.59 ± 0.72	10.22 ± 1.14	10.19 ± 1.18	4a > 4b
(210)	−1.41 ± 1.23	−1.18 ± 0.80	5.28 ± 2.49	2.23 ± 1.99	

Abbreviations: mPFC, medial prefrontal cortex; RSDG, retrosplenial dysgranular and granular cortices.
The effects of sequential nicotine administration on the percentage change observed in peak CBV values relative to the baseline for each of the two injections. The upper and lower values represent the 1st and 2nd injections as shown by the exemplary superscripts a and b, respectively. Significant group differences were thresholded at $p < 0.05$ after Bonferroni correction. Values represent the mean ± SEM for each group.

methiodide and nicotine ($p > 0.5$) (Figure 5b). However, inspection of respective areas under the curves suggested apparent differences in their temporal profiles (Figure 5a). It is important to note that a log–linear regression ANOVA of the peak MAP effects revealed a linear dose–response curve for nicotine ($p = 0.005$) (Figure 5b).

A whole-brain, voxel-wise group analysis using a 2 (DOSE: nicotine methiodide *vs* saline) × 2 (INJECTION) ANOVA indicated no significant rCBV alterations at $p_{\text{corrected}} < 0.005$ (Figure 5c). By comparison, there were large group differences between the saline and nicotine groups as described above. The prominent absence of rCBV changes in the face of a significant vasopressor response to nicotine methiodide supports the interpretation of a direct, central nicotinic-mediated action. In addition, the separation of central and peripheral effects of nicotine is

Table 3 DOSE × INJECTION Interaction on Peak rCBV Responses to Nicotine

Area (number of voxels)	Group				Group differences
	1	2	3	4	
	Saline	0.03 mg/kg	0.10 mg/kg	0.30 mg/kg	
Primary cortex					
Somatosensory	−1.81 ± 0.82[a]	0.39 ± 0.96	12.67 ± 1.25	13.21 ± 1.23	3 > 1, 2; 4 > 1, 2
(253)	−1.42 ± 0.93[b]	−1.29 ± 0.76	5.80 ± 2.64	0.99 ± 2.75	3a > 3b; 4a > 4b
Insula	−1.96 ± 0.98	0.08 ± 1.47	16.49 ± 1.44	14.99 ± 1.09	3 > 1, 2; 4 > 1, 2
(90)	0.50 ± 1.12	−0.80 ± 0.84	7.44 ± 3.45	−0.10 ± 3.10	3a > 3b; 4a > 4b
Motor	−1.74 ± 0.93	−0.32 ± 0.79	13.97 ± 2.13	9.25 ± 1.09	3 > 1, 2; 4 > 1, 2
(150)	0.75 ± 0.94	−0.67 ± 0.40	6.32 ± 2.74	−0.82 ± 2.60	3a > 3b; 4a > 4b
Limbic cortex					
Orbital	−2.13 ± 0.59	−0.66 ± 1.15	12.87 ± 0.99	7.49 ± 1.72	3 > 1, 2, 4; 4 > 1, 2
(104)	0.54 ± ± 0.88	−1.13 ± 0.62	5.40 ± 2.32	−1.36 ± 2.72	3a > 3b; 4a > 4b
Cingulate	−1.01 ± 0.76	0.48 ± 1.11	18.87 ± 2.76	18.26 ± 1.72	3 > 1, 2; 4 > 1, 2
(125)	−1.60 ± 1.20	−0.65 ± 0.81	9.29 ± 3.65	1.55 ± 3.08	2 > 1; 3a > 3b; 4a > 4b
RSDG	−1.81 ± 0.61	0.26 ± 0.63	14.13 ± 2.30	14.52 ± 1.99	3 > 1, 2; 4 > 1, 2
(122)	−1.36 ± 1.01	−1.33 ± 0.48	7.40 ± 3.23	1.40 ± 2.83	3a > 3b; 4a > 4b
Olfactory bulb	−2.07 ± 1.78	−5.70 ± 1.37	9.56 ± 1.42	4.59 ± 1.50	3 > 1, 2; 4 > 1, 2
(35)	0.26 ± 1.78	0.94 ± 1.63	3.89 ± 1.93	−1.96 ± 1.47	2a > 2b; 3a > 3b; 4a > 4b
Thalamus	−2.09 ± 0.31	−0.79 ± 0.63	9.39 ± 1.19	7.52 ± 1.37	3 > 1, 2; 4 > 1, 2
(33)	−0.61 ± 1.01	−0.88 ± 0.76	5.07 ± 2.23	−0.25 ± 1.80	3a > 3b; 4a > 4b

Abbreviations: mPFC, medial prefrontal cortex; RSDG, retrosplenial dysgranular and granular cortices.
ANOVA results of the 4 (DOSE) × 2 (INJECTION) interactions of nicotine administration. Values represent the percentage change observed in peak CBV values relative to each injection baseline. The upper and lower values represent the 1st and 2nd injections as shown by the exemplary superscripts a and b, respectively. Significant group differences were thresholded at $p < 0.05$ after Bonferroni correction. Values represent the mean ± SEM for each group. Note the primary cortical distribution of effects.

substantiated by the distinction between the biphasic dose–effect relationships characterizing nicotine-induced brain activation and the linear dose–effect relationships of its hypertensive effect, suggesting that the two response patterns represent independent mechanisms.

DISCUSSION

Using high-field fMRI measurements of rCBV, a hemodynamic-based surrogate of neuronal activity, in drug-naïve rats together with novel, pharmacokinetic model-driven analyses, we demonstrated marked region- and dose-dependent brain response patterns both to an initial nicotine injection and as a function of acute tolerance development following repeated nicotine administration. Such diverse nicotinic network activation likely reflects the regional distribution and pharmacological properties of multiple nAChR subtypes.

Nicotine-Induced Activation

In general agreement with previous phMRI studies of intravenous nicotine in drug-naïve rats (Choi *et al*, 2006; Gozzi *et al*, 2006) and dependent human smokers (Stein *et al*, 1998), our data show that nicotine induces widespread changes in neuronal activity consistent with the ubiquitous nAChR brain distribution and its diverse behavioral and physiological effects (Dani and Bertrand, 2007; Rose, 2007). These prominent nicotine actions lasted less than 10 min, similar to that reported by other fMRI studies employing bolus intravenous injections (Gotti *et al*, 2006; Stein *et al*, 1998) and within the approximately 5-min efficacy window of drug subjective ratings (eg, drug 'liking') following intravenous and inhaled nicotine in smokers (Henningfield *et al*, 1985). This duration of drug action suggests that human subjective reports are likely associated with specific underlying neural mechanisms.

The utility of phMRI to measure the central effects of nicotine emerges when compared with other regional mapping procedures. Studies using the [C^{14}]2-deoxyglucose (2-DG) accumulation technique reported that the effects of moderate doses of nicotine on cerebral glucose metabolism were restricted to subcortical structures (London *et al*, 1988; McNamara *et al*, 1990; Pontieri *et al*, 1996), whereas widespread effects in cortical areas appeared only with an exceedingly high, 10 mg/kg intraperitoneal dose, suggesting

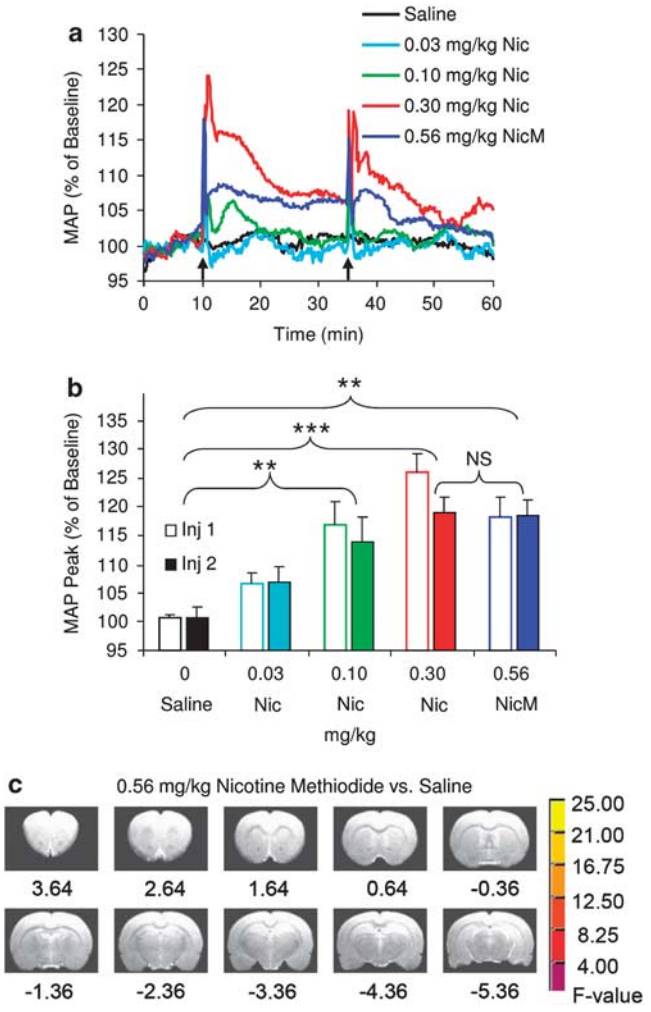

Figure 5 Equimolar doses of nicotine (Nic) and nicotine pyrrolidine methiodide (NicM) produced equivalent increases in peak mean arterial blood pressure (MAP), but the NicM failed to affect relative cerebral blood volume (rCBV). (a) Time courses of the group averaged MAP responses. (b) Peak MAP increases in response to two sequential intravenous injections of saline ($n=6$), nicotine (0.03, 0.1, or 0.3 mg/kg; all $n=4$) and NicM (0.56 mg/kg, $n=5$). Analysis of variance (ANOVA) (5 GROUPS × 2 INJECTIONS) demonstrated only a significant GROUP effect ($p<0.001$). Consequently, comparisons of MAP were based on the group means of the two injections. Significant group differences after Bonferroni correction are indicated: $^{**}p<0.01$ and $^{***}p<0.001$, in comparison to the saline group. There was no statistically significant difference between 0.30 mg/kg Nic and 0.56 mg/kg NicM. (c) Voxel-wise group analysis using a 2 (DOSE: nicotine methiodide *vs* saline) × 2 (INJECTION) ANOVA indicated no significant differences in peak rCBV responses to nicotine methiodide and saline. Voxels in these maps were thresholded by F-statistics for DOSE main effect $p_{corrected}<0.005$.

a possible difference in regional drug sensitivity (McNamara *et al*, 1990). Apparent discrepancies from the current phMRI data may be related to the ability of assessing brain activation almost instantaneously using phMRI *vs* measuring a cumulative change in 2-DG levels over a substantially longer (30–45 min) time period where short duration drug actions may be lost in the temporal 'noise' (see Marota *et al*, 2000). Nevertheless, London *et al* (1988) were able to determine that activation induced by subcutaneous nicotine was short-lived, peaking 2 min after injection and rarely exceeding 15 min in duration. Localizing immediate-early gene (IEG) responses following acute subcutaneous nicotine revealed widespread cortical and subcortical activation (Mathieu-Kia *et al*, 1998; Schochet *et al*, 2005) similar to our phMRI results. More germane to this study, the assessment of single bolus intravenous nicotine injections yielded negative IEG results (Samaha *et al*, 2005), and only with serial intravenous injections did nicotine activate IEGs (Samaha *et al*, 2005; Pich *et al*, 1997). The necessity for repeated injections or sustained administration (subcutaneously, see Schochet *et al*, 2005; prolonged infusions, see Ren and Sagar, 1992) and the persistence of induced ΔFosB have shifted the focus of IEG brain mapping to long-term adaptations that develop after chronic drug use (McClung *et al*, 2004). As an analytical pharmacological tool, phMRI, although still evolving, clearly offers advantages over 2-DG and IEG immunohistochemical techniques in its ability to localize nicotine's acute regional effects, determining its kinetics, and investigating acute tolerance. These advantages are discussed below in the context of these results.

Nicotine-Induced Dose-Dependent and Region-Selective Activation

Acute nicotine administration induced dose-dependent neuronal effects. Although the lowest nicotine dose administered, like saline, induced little change in rCBV, the middle and high doses (0.1 and 0.3 mg/kg) significantly increased activity in many cortical areas, with the largest activation almost always (RSDG being the exception) associated with the middle dose. Furthermore, relative to that dose and consistent with an inverted U-shaped dose–response neuronal function, the highest nicotine dose induced little neuronal activation in NAc, amygdala, and olfactory cortex, and a more limited response in other limbic areas, including the septum, hippocampus, and hypothalamus. These biphasic actions provide a preliminary mechanistic explanation underlying the oft-reported biphasic behavioral and cognitive actions of nicotine, including learning and memory processes (Levin *et al*, 1998, 2006; Levin and Chen, 2004; Matta *et al*, 2007) and locomotor activity (Laviolette *et al*, 2002), which are closely associated with these brain circuits. Reports that nicotine decreased cerebral blood flow in the hippocampus while increasing it in the thalamus and visual cortex in human smokers (Domino *et al*, 2000, 2004; Zubieta *et al*, 2005) are also in accord with these data. In addition, the biphasic nicotine effects observed in this study are consistent with earlier electroencephalographic data, which demonstrated that moderate doses of nicotine increased (ie, stimulant effect), while high doses decreased cortical activation (ie, depressant effect) in human subjects (Ashton *et al*, 1974, 1980) and preclinical studies (Armitage *et al*, 1969; Guha and Pradhan, 1976). Admittedly, the neuroanatomical sources of these electroencephalographic observations remain to be elucidated, although the involvement of the limbic system was implicated (Ashton *et al*, 1980).

The observed dose-dependent and region-specific rCBV activation patterns may provide insight into possible neuropharmacological mechanisms underlying nicotine actions. Among the two main receptor subtypes, $\alpha4\beta2^*$ nAChRs are

widely expressed throughout the brain, whereas receptors containing α7 subunits have a more limited distribution. Furthermore, in contrast to the high-binding affinity (nM) of nicotine for α4β2* nAChRs, which mediate slow decaying currents, nicotine has a lower affinity (μM) for α7* receptors, which mediate fast currents, and are rapidly desensitized *in vitro* (Albuquerque *et al*, 1997; Dani and Bertrand, 2007; Wonnacott, 1986). Our highest nicotine dose reduced neuronal activation relative to the middle dose in limbic regions (eg, hippocampus and septum), which are characterized by a dense expression of α7* subunit-containing nAChRs (Alkondon *et al*, 1996; Azam *et al*, 2003; Clarke *et al*, 1985; Marks *et al*, 1986) and is consistent with the *in vitro* characteristics for this receptor type.

The 0.1 mg/kg nicotine dose might be expected to yield brain nicotine concentrations in the nM range (Maisonneuve *et al*, 1997). At these concentrations, nicotine has presumably activated and subsequently desensitized mainly α4β2* nAChRs, resulting in excitatory effects on principal neurons in widespread brain regions through mechanisms that are still only partially understood (Alkondon *et al*, 2000b; Ji and Dani, 2000; Mansvelder *et al*, 2002). In contrast, nicotine at 0.3 mg/kg might be expected to yield concentrations in the íM range (Rowell and Li, 1997), sufficient to activate and subsequently desensitize both α7* and α4β2* nAChRs as discussed previously (Alkondon *et al*, 2000a; Quick and Lester, 2002). Strong activation of α7* nAChRs (eg, after the high nicotine dose) on limbic system interneurons would likely enhance inhibitory input onto pyramidal neurons (Alkondon *et al*, 2000b; Ji and Dani, 2000), thereby shifting network activity to a depressed state or lower excitatory levels than those associated with 0.1 mg/kg nicotine. In support of this possibility, α7* receptors are found to be most prominent on GABAergic inhibitory interneurons in the hippocampus (Ji and Dani, 2000; Jones and Yakel, 1997), whereas α4β2* nAChRs are the predominant type involved in the modulation of cerebral cortical interneurons that results in inhibition and disinhibition of pyramidal neurons (Alkondon *et al*, 2000b). Fast desensitization of α7* and α4β2* receptors might also account for the shorter duration effects of nicotine at the highest dose (Dani *et al*, 2000; Ochoa *et al*, 1989, 1990) (Tables 2 and 3). As single neurons may express multiple nAChR subtypes, and the regulation of network processes likely engages multiple neurotransmitters and cell types, the mechanisms of nicotine action are expected to be extraordinarily complex. For these reasons, future studies should employ nAChR subtype-selective and regional microinjection-specific drug administration to better understand the circuit processing and behavioral consequences of nicotine.

Curiously, we observed no phMRI response following the lowest (0.03 mg/kg) dose of nicotine, a dose typically employed in rat nicotine self-administration studies (Corrigall and Coen, 1991; Matta *et al*, 2007) and one that we expected might address the reinforcing properties of nicotine. Our anesthetic choice was governed by preliminary studies in which nicotine-induced (0.30 mg/kg) activation acquired under isoflurane anesthesia was both reproducible and qualitatively larger than effects observed using α-chloralose and propofol anesthesia. Nevertheless, findings that anesthesia reduces brain activation produced by nicotinic agonists (Chin *et al*, 2008; Mori *et al*, 2001; Suarez *et al*, 2009; Yamashita *et al*, 2005) might help explain this discrepancy, which may best be addressed using a non-anesthetized rodent model. Although technically more difficult owing to requisite behavioral habituation training, customized coil design, and head-post surgery, phMRI using awake animals holds promise that drug effects on multiple brain pathways may be investigated in the context of relevant behaviors (eg, Li *et al*, 2008).

Development of Tachyphylaxis

Previous direct comparisons of cortical and subcortical nicotine tolerance are rare. *In vitro* studies by Marks *et al* (1993) demonstrated that the magnitude of biochemical tolerance to nicotine varied between cortical and mid-brain tissue following chronic nicotine exposure despite nAChR upregulation and the absence of residual 'chronic' nicotine. The use of phMRI allowed us to assess *in vivo* regional differences in acute tolerance to nicotine at a whole-brain level. Repeated and rapid intravenous nicotine administration produced profound tachyphylaxis in the thalamus along with multiple cortical areas. In contrast, subcortical limbic structures including the septum, amygdala, NAc, and hypothalamus failed to demonstrate significant levels of acute tolerance, even at the highest dose (Table 2 and Figure 2), leading us to speculate that differential receptor desensitization rates, corresponding to different nAChR subtypes, may contribute to such regional tolerance development heterogeneity. *In vivo* studies of recovery from desensitized states have shown slow rates (tens of minutes) for α4β2* receptors (Mansvelder *et al*, 2002) in contrast to the very fast rates for α7* subtypes (Dani *et al*, 2000). Thus, α4β2* receptors may have been desensitized by the first nicotine injection and remained largely in an inactivated state that extended through the 25-min observation interval before the second injection. Consequently, significant tolerance would likely be observed in those regions where α4β2* receptors are the predominate subtype regulating neuronal activity (Alkondon and Albuquerque, 2004; Alkondon *et al*, 2000a).

Consistent with the foregoing notion, significant acute tolerance was found in widespread cortical and subcortical regions that contain a high density of α4β2* receptors and where the expression of α7* receptors is either scarce (eg, thalamus) or restricted within cortical layer VI (Clarke *et al*, 1985). In contrast, it is likely that a large portion of α7* receptors would have recovered from the desensitized (ie, inactivated) state by the time of the second nicotine injection. As such, the general resistance to acute tolerance development seen in the hippocampus, amygdala, septum, NAc, olfactory system, and hypothalamus corresponds to limbic regions with dense α7* nAChRs. Given their known involvement in cognitive functions, the lack of neurophysiological tolerance development to repeated nicotine application in many of these limbic systems may be linked to the lack of tolerance to the cognitive enhancing effects of α7* nAChR agonists demonstrated in several recent *in vivo* preclinical and human studies (see Thomsen *et al*, 2010, for a review).

Similar nAChR regional heterogeneity and selective desensitization could also provide a neuropharmacological explanation for the differential pattern of behavioral tolerance often reported for nicotine (Perkins *et al*, 1994;

Warburton and Mancuso, 1998). The current regional neuronal tolerance heterogeneity is of potential behavioral relevance to the extent that multiple sensory systems, including the thalamus and sensorimotor and insular cortices, support some of the more aversive experiences of nicotine, while the stimulating, positive effect and cognition-enhancing effects of this drug are associated more with its action on the mesolimbic dopamine system (Di Chiara, 2000; Rose, 2007). In smokers, the first 1–2 cigarettes of the day almost completely saturate high-affinity $\alpha4\beta2^*$ nAChRs (Brody *et al*, 2006). Yet, continual nicotine intake, maintained by frequent smoking, may be reinforcing by repeatedly activating limbic sites with abundant non-$\alpha4\beta2^*$ receptors that do not desensitize or remain inactivated to repeated nicotine administration. If replicated and extended, these findings suggest a neurobiological mechanism that underlies the maintenance of smoking behavior during the day and support the necessity of developing smoking cessation aids to target $\alpha7^*$ and other non-$\alpha4\beta2^*$ nAChRs (Rose, 2007).

The presence and development of functional tolerance, particularly with our relatively short inter-injection interval design, requires consideration of the signal baseline status as we normalized each nicotine CBV response to its immediate preinjection baseline period. Before normalization, we first confirmed the absence of motion artifacts (none were expected as the animals were paralyzed and artificially ventilated). The relatively short interval between injections also meant that there was non-metabolized nicotine present in the brain. However, consistent with previous fMRI data (Gotti *et al*, 2006; Stein *et al*, 1998), prominent rCBV responses elicited by nicotine were found to last less than 10 min (Figure 4b and c) and returned to preinjection baseline levels within the 25 min observation intervals. Moreover, the paired nicotine administration paradigm used in this study serves as a valid model to study tolerance during continued cigarette smoking in dependent smokers and nicotine self-administration in preclinical models. Considering the different nicotine plasma half-life in rats (50 min) and human beings (2 h), the 25 min interval between paired nicotine injections is closely analogous to the typical 45 min to 1 h cigarette *ad libitum* intervals in smokers. Consequently, the presence of residual nicotine in this study is likely similar to that which occurs in smokers, who continue to smoke frequently after the first cigarette of the day.

Nicotine-Induced Brain Activation Is Independent of Its Peripheral Effects

Nicotine methiodide produced no measurable brain activation, while it increased peak MAP at a magnitude comparable to an equimolar dose of nicotine (Figures 5a and b), arguing that nicotine-induced neuronal activation, manifested as changes in rCBV, most likely resulted from interactions with neuronal nAChRs rather than indirectly via peripheral receptor-mediated effects such as increased blood pressure. Gozzi *et al* (2006) and Suarez *et al* (2009) also have argued that nicotine-induced, region-specific activation measured by BOLD or CBV does not result from generalized cerebral vasodilatation involving cholinergic pathways (Sato *et al*, 2002). This is important as it has been suggested that nicotinic activation could, either via a direct vasodilatory action or by releasing acetylcholine, increase regional CBF in the hippocampus and cortex, independent of regional metabolism, through projection of basal forebrain cholinergic fibers (Sato *et al*, 2002, 2004). Any substantial contribution to hemodynamic-based phMRI changes observed in the present and previous research in response to nicotine via a vasodilatory mechanism has yet to be determined. Nevertheless, it is difficult to explain how nicotine can differentially activate and desensitize cortical and subcortical limbic regions through this signaling pathway alone. Future research should examine potential regional differences in vasculature and neurovascular coupling (Sloan *et al*, 2010) that might account for, at least in part, the differential rCBV changes seen in cortical and subcortical limbic areas. Further, the negative nicotine methiodide data lend support to the notion that CBV changes mirror direct neuronal nAChR activation, consistent with the ubiquitous distribution of nicotinic receptors in the brain and their functional properties in synaptic transmission.

In conclusion, we demonstrated that nAChR activation, particularly at higher nicotine doses, produces differential or even opposite effects on neuronal activity in cortical and subcortical limbic networks. The marked regional heterogeneity in acute tolerance in brain response to nicotine may be relevant to neurobiological mechanisms underlying differential tolerance profiles across behavioral domains associated with the rewarding properties of frequent tobacco consumption. These diverse effects of nicotinic activation also pose important challenges both for the development of effective nicotinic therapeutic agents and for dosing strategies to treat nicotine addiction and neurological diseases involving nicotinic transmission deficits (Dome *et al*, 2010; Thomsen *et al*, 2010). In light of these results, new approaches, including allosteric modulation of nAChRs, should be explored to circumvent development of acute tolerance, especially in crucial brain networks, resulting from the use of conventional nicotinic agents (Maelicke and Albuquerque, 1996). Future studies using agonists and antagonists selective for particular nAChR subtypes might help clarify the effects of activation and desensitization of these receptor subtypes on brain activity.

ACKNOWLEDGEMENTS

This research was funded by the US National Institutes of Health, National Institute on Drug Abuse, and Intramural Research Program. We thank Pradeep Kurup, MS and Tom Ross, PhD for their statistical assistance.

DISCLOSURE

The authors declare no conflict of interest.

REFERENCES

Aceto MD, Awaya H, Martin B, May EL (1983). Antinociceptive action of nicotine and its methiodide derivatives in mice and rats. *Br J Pharmacol* **79**: 869–876.

Albuquerque EX, Alkondon M, Pereira EFR, Castro NG, Schrattenholz A, Barbosa CT *et al* (1997). Properties of neuronal nicotinic acetylcholine receptors: pharmacological characterization and modulation of synaptic function. *J Pharmacol Exp Ther* **280**: 1117–1136.

Albuquerque EX, Pereira EFR, Alkondon M, Rogers SW (2009). Mammalian nicotinic acetylcholine receptors: from structure to function. *Physiol Rev* **89**: 73–120.

Alkondon M, Albuquerque EX (2004). The nicotinic acetylcholine receptor subtypes and their function in the hippocampus and cerebral cortex. *Prog Brain Res* **145**: 109–120.

Alkondon M, Pereira EFR, Almeida LEF, Randall WR, Albuquerque EX (2000a). Nicotine at concentrations found in cigarette smokers activates and desensitizes nicotinic acetylcholine receptors in CA1 interneurons of rat hippocampus. *Neuropharmacology* **39**: 2726–2739.

Alkondon M, Pereira EFR, Eisenberg HM, Albuquerque EX (2000b). Nicotinic receptor activation in human cerebral cortical interneurons: a mechanism for inhibition and disinhibition of neuronal networks. *J Neurosci* **20**: 66–75.

Alkondon M, Rocha ES, Maelicke A, Albuquerque EX (1996). Diversity of nicotinic acetylcholine receptors in rat brain. V. α-Bungarotoxin-sensitive nicotinic receptors in olfactory bulb neurons and presynaptic modulation of glutamate release. *J Pharmacol Exp Ther* **278**: 1460–1471.

Armitage AK, Hall GH, Sellers CM (1969). Effects of nicotine on electrocortical activity and acetylcholine release from cat cerebral cortex. *Br J Pharmacol* **35**: 152–160.

Ashton H, Marsh VR, Millman JE, Rawlins MD, Telford R, Thompson JW (1980). Biphasic dose-related responses of the CNV (contingent negative variation) to I.V. Nicotine in man. *Br J Clin Pharmacol* **10**: 579–589.

Ashton H, Millman JE, Telford R, Thompson JW (1974). The effects of caffeine, nitrazepam and cigarette smoking on the contingent negative variation in man. *Electroenceph Clin Neurophysiol* **37**: 59–71.

Azam L, Winzer-Serhan W, Leslie FM (2003). Co-expression of α7 and β2 nicotinic acetylcholine receptor subunit mRNA within rat brain cholinergic neurons. *Neuroscience* **119**: 965–977.

Barlow RB, Dobson NA (1955). Nicotine monomethiodide. *J Pharm Pharmacol* **7**: 27–34.

Brody AL, Mandelkern MA, London ED, Olmstead RE, Farahi J, Scheibal D *et al* (2006). Cigarette smoking saturates brain $\alpha_4\beta_2$ nicotinic acetylcholine receptors. *Arch Gen Psychiatry* **63**: 907–915.

Chin C-L, Pauly JR, Surber BW, Skoubis PD, Mcgaraughty S, Hradil VP *et al* (2008). Pharmacological MRI in awake rats predicts selective binding of α4β2 nicotinic receptors. *Synapse* **62**: 159–168.

Choi JK, Mandeville JB, Chen YI, Kim YR, Jenkins BG (2006). High resolution spatial mapping of nicotine action using pharmacologic magnetic resonance imaging. *Synapse* **60**: 152–157.

Clarke PB, Schwartz RD, Paul SM, Pert CB, Pert A (1985). Nicotinic binding in rat brain: autoradiographic comparison of [^{3}H]acetylcholine, [^{3}H]nicotine, and [^{125}I]-alpha-bungarotoxin. *J Neurosci* **5**: 1307–1315.

Corrigall WA, Coen KM (1989). Nicotine maintains robust self-administration in rats on a limited-access schedule. *Psychopharmacology* **99**: 473–478.

Corrigall WA, Coen KM (1991). Selective dopamine antagonists reduce nicotine self-administration. *Psychopharmacology* **104**: 171–176.

Cox RW (1996). AFNI: software for analysis and visualization of functional magnetic resonance neuroimages. *Comput Biomed Res* **29**: 162–173.

Dani JA, Bertrand D (2007). Nicotinic acetylcholine receptors and nicotinic cholinergic mechanisms of the central nervous system. *Ann Rev Pharmacol Toxicol* **47**: 699–729.

Dani JA, Radcliffe KA, Pidoplichko VI (2000). Variations in desensitization of nicotinic acetylcholine receptors from hippocampus and midbrain dopamine areas. *Eur J Pharmacol* **393**: 31–38.

Di Chiara G (2000). Role of dopamine in the behavioral actions of nicotine related to addiction. *Eur J Pharmacol* **393**: 295–314.

Dome P, Lazary J, Kalapos MP, Rihmer Z (2010). Smoking, nicotine and neuropsychiatric disorders. *Neurosci Biobehav Rev* **34**: 295–342.

Domino EF, Minoshima S, Guthrie S, Ohl L, Ni L, Koeppe RA *et al* (2000). Nicotine effects on regional cerebral blood flow in awake, resting tobacco smokers. *Synapse* **38**: 313–321.

Domino EF, Ni L, Xu Y, Koeppe RA, Guthrie S, Zubieta JK (2004). Regional cerebral blood flow and plasma nicotine after smoking tobacco cigarette. *Prog Neuro-Psychopharmacol Biol Psychiatry* **28**: 319–327.

Gotti C, Zoli M, Clementi F (2006). Brain nicotinic acetylcholine receptors: native subtypes and their relevance. *Trends Pharmacol Sci* **27**: 482–491.

Gozzi A, Schwarz A, Reese T, Bertani S, Crestan V, Bifone A (2006). Region-specific effects of nicotine on brain activity: a pharmacological MRI study in the drug-na¿ve rat. *Neuropsychopharmacology* **31**: 1690–1703.

Guha D, Pradhan SN (1976). Effects of nicotine on EEG and evoked potentials and their interactions with autonomic drugs. *Neuropharmacology* **15**: 225–232.

Henningfield JE, Miyasato K, Jasinski DR (1985). Abuse liability and pharmacodynamic characteristics of intravenous and inhaled nicotine. *J Pharmacol Exp Ther* **234**: 1–12.

Ji D, Dani JA (2000). Inhibition and disinhibition of pyramidal neurons by activation of nicotinic receptors on hippocampal interneurons. *J Neurophysiol* **83**: 2682–2690.

Jones S, Yakel JL (1997). Functional nicotinic ACh receptors on interneurons in the rat hippocampus. *J Physiol (Lond)* **504**: 603–610.

Laviolette SR, Alexson TO, van der Krooy D (2002). Lesions of the tegmental pedunculopontine nucleus block the rewarding effects and reveal the aversive effects of nicotine in the ventral tegmental area. *J Neurosci* **22**: 8653–8660.

Le Foll BE, Goldberg SE (2005). Nicotine induces conditioned place preferences over a large range of doses in rats. *Psychopharmacology* **178**: 481–492.

Le Foll B, Wertheim C, Goldberg SR (2007). High reinforcing efficacy of nicotine in non-human primates. *PLoS One* **2**: e230.

Leslie RA, James MF (2000). Pharmacological magnetic resonance imaging: a new application for functional MRI. *TiPS* **21**: 314–318.

Levin ED, Bettegowda C, Weaver T, Christopher NC (1998). Nicotine–dizocilpine interactions and working and reference memory performance of rats in the radial-arm maze. *Pharmacol Biochem Behav* **61**: 335–340.

Levin ED, Chen E (2004). Nicotinic involvement in memory function in zebrafish. *Neurotoxicol Teratol* **26**: 731–735.

Levin ED, McClernon FJ, Rezvani AH (2006). Nicotinic effects on cognitive function: behavioral characterization, pharmacological specification and anatomic localization. *Psychopharmacology* **184**: 523–539.

Li Z, DiFranza JR, Wellman RJ, Kulkarni P, King JA (2008). Imaging brain activation in nicotine-sensitized rats. *Brain Res* **1199**: 91–99.

Logothetis NK, Pauls J, Augath M, Trinath T, Oeltermann A (2001). Neurophysiological investigation of the basis of the fMRI signal. *Nature* **412**: 150–157.

London ED, Connolly RJ, Szikszay M, Wamsley JK, Dam M (1988). Effects of nicotine on local cerebral glucose utilization in the rat. *J Neurosci* **8**: 3920–3928.

Lu H, Patel S, Luo F, Li SJ, Hillard CJ, Ward BD *et al* (2004). Spatial correlations of laminar BOLD and CBV responses to rat whisker

stimulation with neuronal activity localized by Fos expression. *Magn Reson Med* **52**: 1060–1068.
Lu H, Scholl CA, Zuo Y, Demny S, Rea W, Stein EA *et al* (2010). Registering and analyzing rat fMRI data in the stereotaxic framework by exploiting intrinsic anatomical features. *Magn Reson Imaging* **28**: 146–152.
Lu H, Scholl CA, Zuo Y, Stein EA, Yang Y (2007). Quantifying BOLD effect in CBV-weighted fMRI at 9.4T. *Magn Reson Med* **58**: 616–621.
Lu H, Yang S, Zuo Y, Demny S, Stein EA, Yang Y (2008). Real-time animal fMRI and its application to neuropharmacological studies. *Magn Reson Imaging* **26**: 1266–1272.
Maelicke A, Albuquerque EX (1996). New approach to drug therapy in Alzheimer's disease. *Drug Disc Today* **1**: 53–59.
Maisonneuve IM, Mann GL, Deibel CR, Glick SD (1997). Ibogaine and the dopaminergic response to nicotine. *Psychopharmacology* **129**: 249–256.
Mandeville JB, Marota JJ, Kosofsky BE, Keltner JR, Weissleder R, Rosen BR *et al* (1998). Dynamic functional imaging of relative cerebral blood volume during rat forepaw stimulation. *Magn Reson Med* **39**: 615–624.
Mansvelder HD, Keath JR, McGehee DS (2002). Synaptic mechanisms underlie nicotine-induced excitability of brain reward areas. *Neuron* **33**: 905–919.
Marks MJ, Grady SR, Collins AC (1993). Downregulation of nicotinic receptor function after chronic nicotine infusion. *J Pharmacol Exp Ther* **266**: 1268–1276.
Marks MJ, Stitzel JA, Romm E, Weher JM, Collins AC (1986). Nicotinic binding sites in the rat and mouse brain: comparison of acetylcholine, nicotine and α-bungarotoxin. *Mol Pharmacol* **30**: 427–436.
Marota JA, Mandeville JB, Weisskoff RM, Moskowitz MA, Rosen BR, Kosofsky BE (2000). Cocaine activation discriminates dopaminergic projections by temporal response: an fMRI study in rat. *NeuroImage* **11**: 13–23.
Martin C, Sibson NR (2008). Pharmacological MRI in animals: a useful tool for 5-HT research? *Neuropharmacology* **55**: 1038–1047.
Mathieu-Kia AM, Pages C, Besson M-J (1998). Inducibility of c-Fos protein *in visuo*-motor system and limbic structures after acute and repeated administration of nicotine n the rat. *Synapse* **29**: 33–354.
Matta SG, Balfour DJ, Benowitz NL, Boyd RT, Buccafusco JJ, Caggiula AR *et al* (2007). Guidelines on nicotine dose selection for *in vivo* research. *Psychopharmacology* **190**: 269–319.
McClung CA, Ulery PG, Perrotti LI, Zachariou V, Berton O, Nestler EJ (2004). ΔFosB: a molecular switch for long-term adaptation in the brain. *Mol Brain Res* **132**: 146–154.
McNamara D, Larson DM, Rapoport SI, Soncrant TT (1990). Preferential metabolic activation of subcortical brain areas by acute administration of nicotine to rats. *J Cereb Blood Flow Metab* **10**: 48–56.
Mendelson JH, Goletiani N, Sholar MB, Siegel AJ, Mello NK (2008). Effects of smoking successive low- and high-nicotine cigarettes on hypothalamic-pituitary-adrenal axis hormones and mood in men. *Neuropsychopharmacology* **33**: 749–760.
Moore C, Yang Y, Ramage AG (2008). Cardiovascular effects of activation of central α7 and α4β2nAChRs: a role for vasopressin in anaesthetized rats. *Br J Pharmacol* **153**: 1728–1738.
Mori T, Zhao X, Zou Y, Aistrup GL, Nishikawa K, Marszalec W *et al* (2001). Modulation of neuronal nicotinic acetylcholine receptors by halothane in rat cortical neurons. *Mol Pharmacol* **59**: 732–743.
Newhouse PA, Potter A, Levin ED (1997). Nicotinic system involvement in Alzheimer's and Parkinson's diseases. Implications for therapeutics. *Drugs Aging* **11**: 206–228.
Ochoa EL, Chattopadhyay A, McNamee MG (1989). Desensitization of the nicotinic acetylcholine receptor: molecular mechanisms and effect of modulators. *Cell Mol Neurobiol* **9**: 141–178.
Ochoa EL, Li L, McNamee MG (1990). Desensitization of central cholinergic mechanisms and neuroadaptation to nicotine. *Mol Neurobiol* **4**: 251–287.
Paxinos G, Watson C (2005). *The Rat Brain in Stereotactic Coordinates* 5th edn. Academic Press: San Diego, CA.
Perkins KA (2002). Chronic tolerance to nicotine in humans and its relationship to tobacco dependence. *Nicotine Tob Res* **4**: 405–422.
Perkins KA, Grobe JE, Epstein LH, Caggiula AC, Stiller RL, Jacob RG (1993). Chronic and acute tolerance to subjective effects of nicotine. *Pharmacol Biochem Behav* **45**: 375–381.
Perkins KA, Grobe JE, Fonte C, Goettler J, Caggiula AR, Reynolds WA *et al* (1994). Chronic and acute tolerance to subjective, behavioral and cardiovascular effects of nicotine in humans. *J Pharmacol Exp Ther* **270**: 628–638.
Perry E, Martin-Ruiz C, Lee M, Griffiths M, Johnson M, Piggott M *et al* (2000). Nicotinic receptor subtypes in human brain ageing, Alzheimer and Lewy body diseases. *Eur J Pharmacol* **393**: 215–222.
Pich, EM, Pagliusi SR, Tessari M, Talabot-Ayer D, van Huijsduijnen RH *et al* (1997). Common neural substrates for the addictive properties of nicotine and cocaine. *Science* **275**: 83–86.
Pomerleau OF, Collins AC, Shiffman S, Pomerleau CS (1993). Why some people smoke and other do not: new perspectives. *J Counsel Clin Psychol* **61**: 723–731.
Pontieri FE, Tanda G, Orzi F, Di Chiara G (1996). Effects of nicotine on the nucleus accumbens and similarity to those of addictive drugs. *Nature* **382**: 255–258.
Quick MW, Lester RAJ (2002). Desensitization of neuronal nicotinic receptors. *J Neurobiol* **53**: 457–478.
Ren T, Sagar SM (1992). Induction of c-*fos* immunostaining in the rat brain after the systemic administration of nicotine. *Brain Res Bull* **29**: 589–597.
Rose JE (2007). Multiple brain pathways and receptors underlying tobacco addiction. *Biochem Pharmacol* **74**: 1263–1270.
Rowell PP, Li M (1997). Dose–response relationship for nicotine-induced up-regulation of rat brain nicotinic receptors. *J Neurochem* **68**: 1982–1989.
Samaha A-N, Yau W-Y W, Yang P, Robinson TE (2005). Rapid delivery of nicotine promotes behavioral sensitization and alters its neurobiological impact. *Biol Psychiatry* **57**: 351–360.
Sato A, Sato Y, Uchida S (2002). Regulation of cerebral cortical blood flow by the basal forebrain cholinergic fibers and aging. *Auton Neurosci Basic Clin* **96**: 13–19.
Sato A, Sato Y, Uchida S (2004). Activation of the intracerebral cholinergic nerve fibers originating in the basal forebrain increases regional cerebral blood flow in the rat's cortex and hippocampus. *Neurosci Lett* **361**: 90–93.
Schochet TL, Kelley AE, Landry CF (2005). Differential expression of arc mRNA and other plasticity-related genes induced by nicotine in adolescent rat forebrain. *J Neurosci* **135**: 285–297.
Sheth S, Nemoto M, Guiou M, Walker M, Pouratian N, Toga AW (2003). Evaluation of coupling between optical intrinsic signals and neuronal activity in rat somatosensory cortex. *NeuroImage* **19**: 884–894.
Sloan HL, Austin VC, Blamire AM, Schnupp JWH, Lowe AS, Allers KA *et al* (2010). Regional differences in neurovascular coupling in rat brain as determined by fMRI and electrophysiology. *NeuroImage* **53**: 399–411.
Smith AJ, Blumenfeld H, Behar KL, Rothman DL, Shulman RG, Hyder F (2002). Cerebral energetic and spiking frequency: the neurophysiological basis of fMRI. *Proc Natl Acad Sci USA* **99**: 10765–10770.
Sorge RE, Clarke PBS (2009). Rats self-administer intravenous nicotine delivered in a novel smoking-relevant procedure: effects of dopamine antagonists. *J Pharmacol Exp Ther* **330**: 633–640.

Stein EA, Pankiewicz J, Harsch HH, Cho J-K, Fuller S A, Hoffman *et al* (1998). Nicotine-induced limbic cortical activation in the human brain: a functional MRI study. *Am J Psychiatry* **155**: 1009–1015.

Suarez SV, Amadon A, Giacomini E, Wiklund A, Changeux JP, Le Bihan D *et al* (2009). Brain activation by short-term nicotine exposure in anesthetized wild-type and beta2-nicotinic receptors knockout mice: a BOLD fMRI study. *Psychopharmacology* **202**: 599–610.

Thomsen MS, Hansen HH, Timmerman DB, Mikkelsen JD (2010). Cognitive improvement by activation of α_7 nicotinic acetylcholine receptors: from animal models to human pathophysiology. *Curr Pharm Des* **16**: 323–343.

Vallejo YF, Buisson B, Bertrand D, Green WN (2005). Chronic nicotine exposure upregulates nicotinic receptors by a novel mechanism. *J Neurosci* **25**: 5563–5572.

Warburton DM, Mancuso G (1998). Evaluation of the information processing and mood effects of a transdermal nicotine patch. *Psychopharmacology* **135**: 305–310.

Wonnacott S (1986). Alpha-bungarotoxin binds to low-affinity nicotine binding sites in rat brain. *J Neurochem* **47**: 1706–1712.

Yamashita M, Mori T, Nagata K, Yeh JZ, Narahashi T (2005). Isoflurane modulation of neuronal nicotinic acetylcholine receptors expressed in human embryonic kidney cells. *Anesthesiology* **102**: 76–84.

Zubieta J-K, Heitzeg MM, Xu Y, Koeppe RA, Ni L, Guthrie S *et al* (2005). Regional cerebral blood flow responses to smoking in tobacco smokers after overnight abstinence. *Am J Psychiatry* **162**: 567–577.

Supplementary Information accompanies the paper on the Neuropsychopharmacology website (http://www.nature.com/npp)